

# Anodized 20 nm diameter nanotubular titanium for improved bladder stent applications

Ece Alpaslan<sup>1</sup>  
Batur Ercan<sup>2</sup>  
Thomas J Webster<sup>2,3</sup>

<sup>1</sup>Faculty of Engineering and Natural Sciences, Sabanci University, Istanbul, Turkey; <sup>2</sup>School of Engineering,

<sup>3</sup>Department of Orthopedics, Brown University, Providence, RI, USA

**Abstract:** Materials currently used for bladder applications often suffer from incomplete coverage by urothelial cells (cells that line the interior of the bladder and ureter) which leads to the continuous exposure of the underlying materials aggravating an immune response. In particular, a ureteral (or sometimes called an ureteric or bladder) stent is a thin tube inserted into the ureter to prevent or treat obstruction of urine flow from the kidney. The main complications with ureteral stents are infection and blockage by encrustation, which can be avoided by promoting the formation of a monolayer of urothelial cells on the surface of the stent. Nanotechnology (or the use of nanomaterials) may aid in urothelialization of bladder stents since nanomaterials have been shown to have unique surface energetics to promote the adsorption of proteins important for urothelial cell adhesion and proliferation. Since many bladder stents are composed of titanium, this study investigated the attachment and spreading of human urothelial cells on different nanotextured titanium surfaces. An inexpensive and effective scaled up anodization process was used to create equally distributed nanotubular surfaces of different diameter sizes from 20–80 nm on titanium with lengths approximately 500 nm. Results showed that compared to untreated titanium stents and 80 nm diameter nanotubular titanium, 20 nm diameter nanotubular titanium stents enhanced human urothelial cell adhesion and growth up to 3 days in culture. In this manner, this study suggests that titanium anodized to possess nanotubular surface features should be further explored for bladder stent applications.

**Keywords:** anodization, nanotube, urothelial cells, bladder applications, titanium

## Introduction

Ureteral stents are used to ensure the patency of the ureter, which may be compromised, for example, by a kidney stone or tumor.<sup>1</sup> Ureteral stents may be inserted temporarily or permanently to prevent damage to a blocked kidney. Indwelling times of 12 months or longer are frequently used to hold a ureter open, which may be compressed by tumors in or near the ureter.<sup>1</sup> In many cases, these tumors are inoperable and the stents are used to ensure drainage of urine through the ureter. If urine drainage is compromised for longer periods of time, the kidney can be damaged due to elevated hydrostatic pressure.<sup>1</sup> Stents may also be placed in a ureter that has been irritated or scratched during ureteroscopy, which involves the removal of a stone.<sup>1</sup>

Complications with ureteral stents are dislocation, infection, and blockage by encrustation.<sup>2</sup> There have been some attempts to reduce encrustation of such bladder stents, for example, it was recently shown that coating stents with heparin may reduce infection and encrustation.<sup>2</sup> Other complications can include increased urgency and frequency of urination, blood in the urine, leakage of urine, pain in the kidney, bladder,

Correspondence: Thomas J Webster  
School of Engineering and Department  
of Orthopaedics, Brown University,  
Providence, RI 02917 USA  
Tel +1 401 863 2318  
Fax +1 401 863 2323  
Email thomas\_webster@brown.edu

or groin, and pain in the kidneys during, and for a short time after, urination.<sup>2</sup> While some of these complications are only temporary for stents not implanted for long periods of time, stents permanently implanted may suffer from such continuous problems.

It is commonly recognized that ureteral stent function can be improved by using materials that promote the density and function of urothelial cells (cells that line the interior of the bladder and ureter) since such cells will block immune cells and bacteria from interacting with the underlying foreign synthetic stent.<sup>1-3</sup>

Thus, to improve urethelial cell coverage of the underlying stent, several efforts are underway, such as altering the stent surface properties either by changing the surface chemistry and/or surface roughness.<sup>1-3</sup> While modifying stent surface chemistry will alter stent surface energetics to control initial protein adsorption events important for promoting urothelial cell functions, some researchers have stayed away from such efforts since they will require extensive regulatory pathways.<sup>4</sup> In contrast, modifying the surface roughness of existing stent chemistries (such as titanium) may also alter surface energetics to promote initial protein adsorption events important for increasing urothelial cell functions without requiring extensive regulatory pathways.

Along these lines, nanotechnology (or the use of materials with at least one dimension less than 100 nm) has emerged as a promising new research direction for increasing the efficacy of numerous medical devices.<sup>3-14</sup> This is because nanomaterials mimic the natural nanometer roughness of tissues (such as the bladder and the ureter). The building blocks of life, such as proteins, nucleic acids, lipids, and carbohydrates, are all examples of materials that possess unique properties determined by the size, folding, and patterns at the nanoscale. Moreover, nanoscale surface features on materials can control surface energetics to control cell responses.<sup>3,4</sup>

To improve the performance of titanium for ureter stent applications, here, titanium was anodized to possess nanotubular surface features. Nanotubular titanium prepared by anodization has been investigated for a wide range of medical applications including most prominently orthopedic and vascular applications.<sup>4</sup> To test the biocompatibility of these modified titanium stents, the adhesion and proliferation of human urothelial cells were completed for up to 3 days in culture. Results provided significant evidence that modifying titanium to possess unique nanoscale surface features through anodization (specifically, 20 nm diameter tubes) increased urothelial cell density and should be further explored for ureter stent applications.

## Experimental procedures

### Sample preparation

10 cm × 10 cm, 99.5% pure and annealed titanium foils (0.25 mm thick) were purchased (Alfa Aesar, Ward Hill, MA, USA) and cut into 5 cm × 5 cm squares. Then, each side of these squares was sonicated (VWR 75D) for 1 hour using a cleaning solution (Branson, Phillipsburg, NJ, USA), followed by 30 minutes of sonication with acetone (Mallinckrodt Chemicals, Phillipsburg, NJ, USA), 70% ethanol, and ddH<sub>2</sub>O. These cleaned samples were termed 'conventional titanium' in the present study.

Afterwards, the cleaned titanium samples were etched with a 1.5% HF/1.5% HNO<sub>3</sub> solution (Mallinckrodt Chemicals) for 1 min to remove the oxide layer. This was followed by an anodization process (Figure 1). For anodization, titanium samples were connected to a DC-powered electrochemical cell which had a two-electrode configuration. A 5 cm × 5 cm platinum mesh was used as the cathode and a titanium specimen was used as the anode. The platinum mesh and titanium samples were connected to a DC power supply (3645A DC power supply, Circuit Specialists, Inc., Mesa, AZ, USA) through copper wires. Constant voltages of 20 V and 5 V were applied for 20 min and 40 min, respectively. During anodization, the anode and platinum cathode were kept at a distance of 2.5 cm from each other. The electrolyte solution used in this study was a 0.5% hydrofluoric acid solution and the anodization was conducted inside a Teflon beaker. During anodization, the electrolyte solution was constantly stirred with magnetic agitation to reduce

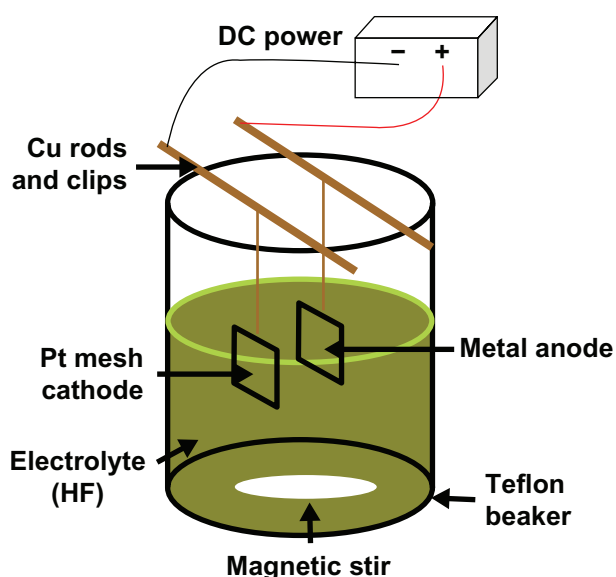


**Figure 1** Schematic of the anodization system.  
Abbreviation: HF, hydrofluoric acid.

the thickness of the double layer at the metal–electrode interface to obtain uniform local current densities on the titanium electrode.

After anodization, the specimens were cut into 1 cm × 1 cm pieces and cleaned with acetone and 70% ethanol for 30 min each. These samples were termed ‘anodized nanotubular titanium’ since, as will be shown, titanium anodized in this manner possesses nanotubes penetrating the titanium surfaces up to 500 nm.<sup>4</sup>

## Sample characterization

### Scanning electron microscopy

Surface characterization of the specimens was conducted with a LEO 1530 VP FE- 4800 field-emission scanning electron microscope (SEM) (Zeiss, Peabody, MA, USA). A 5 kV accelerating voltage was chosen for SEM analysis and the micrographs were captured using secondary electrons collected with an in-lens detector. No sputtering was used to image the surfaces of the conventional or anodized nanotubular titanium substrates.

### Atomic force microscopy

For surface roughness measurements, an Asylum Research atomic force microscope (AFM) (Santa Barbara, CA, USA) was used to scan the conventional and anodized nanotubular titanium substrates. Each sample was analyzed in ambient air under non-contact mode using a silicone ultrasharp cantilever (probe tip radius of 10 nm; MikroMasch, Wilsonville, OR, USA). 1 × 1 μm AFM fields were analyzed and the scan rate was chosen as 1 Hz. Image analysis software (IgorPro, Lake Oswego, OR, USA) was used to generate micrographs and to quantitatively compare the root-mean-square roughness (RMS) of the conventional and anodized nanotubular titanium substrates. RMS is the estimated standard deviation of the bidimensional Gaussian-type distribution of heights around the mean value of the collected points. It is determined using the standard definition:

$$R_q = \sqrt{\frac{1}{n} \left( \sum_{i=1}^n (z_i - \bar{z})^2 \right)}, \quad (1)$$

where  $\bar{z}$  = mean  $z$  height.

### Electron spectroscopy for chemical analysis

For chemical analysis of the top surface layer of the conventional and anodized nanotubular titanium, electron spectroscopy for chemical analysis (ESCA) was performed

using a PerkinElmer 5500 Multitechnique Surface Analyzer System (Waltham, MA, USA). An aluminum K-alpha monochromatized X-ray source was used to stimulate photoemission of the inner shell electrons on the surfaces. The energy of these electrons was then recorded and analyzed for both substrates. Wide scans of both conventional and anodized nanotubular titanium were used to generate low-resolution spectra to identify and quantify the percentage of different elements up to a depth of 10 nm.

## Cell culture

Human urothelial cells (population number 2, ScienCell, 4320 [ScienCell Research Laboratories, Carlsbad, CA, USA]) were cultured in urothelial cell culture medium (ScienCell, 4321; UCM). The media used in these studies was supplemented with 1% urothelial cell growth supplement (UCGS, ScienCell) and 1% penicillin/streptomycin (P/S, ScienCell) as suggested by the vendor and cells were cultured under standard culture conditions (5% CO<sub>2</sub>/95% air at 37°C).

For the 4-hour adhesion assay, a seeding density of 3500 cell/cm<sup>2</sup> was used and for the 3-day proliferation experiments, a seeding density of 2000 cell/cm<sup>2</sup> was used. For the cell experiments, all samples were sterilized using 70% ethanol and UV light for 30 min and 4 hours, respectively. Cells for both the adhesion and proliferation experiments were seeded onto specimens with the media that was supplemented with 10% fetal bovine serum and 1% P/S. For the proliferation experiments, the cell culture media was refreshed with one supplement of 1% UCGS and 1% P/S after 4 hours.

At the end of the prescribed time period, specimens were gently rinsed in a phosphate buffered saline buffer solution to remove non-adherent cells. Then, adherent cells were fixed with 4% formaldehyde (Fisher Scientific, Pittsburgh, PA, USA) for 10 min and nuclei stained by soaking in a 1% DAPI fluorescent dye (Sigma-Aldrich, St Louis, MO, USA) for 15 min. Cell densities were counted in situ from five randomly selected, non-intersecting areas on each specimen under a fluorescence microscope (Leica DM 5500B).

## Statistical analyses

Numerical data were analyzed using standard analysis of variance (ANOVA) followed by Student *t*-tests. All cell experiments were repeated three times both for conventional and anodized nanotubular titanium samples.

## Results and discussion

Research has demonstrated that the inner diameter and the depth of the nanotubes change depending on the type and the concentration of the electrolyte, duration and intensity of the applied voltage, as well as the composition of the alloy used during anodization.<sup>4,18</sup> It can be observed from the SEM images from this study that titanium anodized at 5 V for 40 min resulted in 20 nm diameter nanotubular structures while titanium anodized at 20 V for 20 min resulted in 80 nm nanotubular structures (Figure 2).

Figure 3 and Table 1 provide AFM data concerning the topographical differences between the titanium specimens of interest to the present study. For the conventional titanium, the AFM RMS roughness was  $6.54 \pm 0.37$  nm, while for the 20 nm nanotubular titanium it was  $9.97 \pm 0.83$  nm and for the 80 nm nanotubular it was  $9.01 \pm 0.40$  nm (Table 1). These

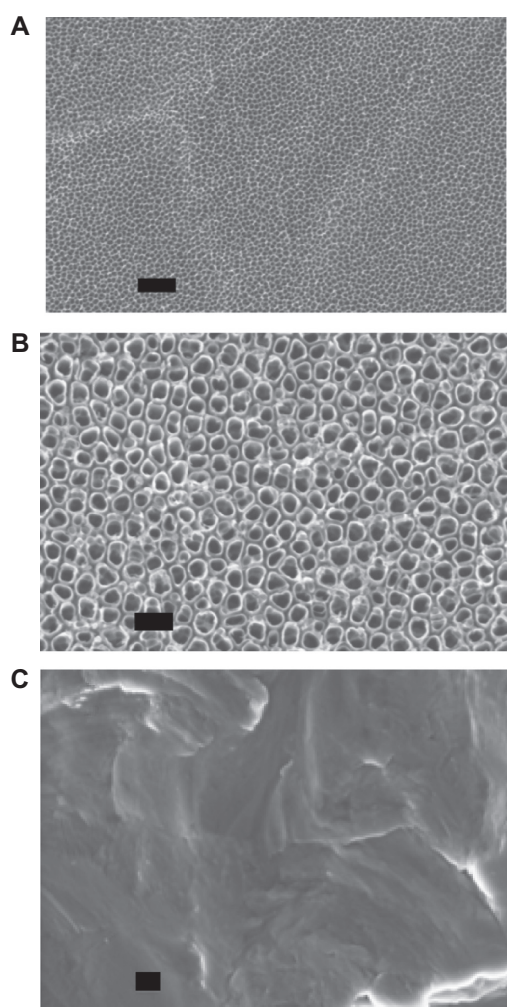


**Figure 2** Scanning electron microscope micrographs of **A**) 20 nm and **B**) 80 nm anodized nanotubular titanium, as well as **C**) conventional titanium. Scale bars = 200 nm.

results indicated that compared to conventional titanium, the anodized nanotubular titanium substrates were more rough at the nanoscale. When the RMS values for micron topographies were compared, no significant differences were observed between 20 nm diameter, 80 nm diameter, and conventional titanium, signifying that the anodization process did not create micron-topographical differences (whereas it did create nanotopographical differences).

Chemical analysis of the samples of interest to the present study were completed by high resolution ESCA. Different ESCA peaks for conventional and anodized nanotubular titanium plates appeared due to the different chemistries from the oxide layer formed on the conventional and anodized titanium. Specifically, O1s, Ti2p3, C1s, Ti3p, and C2s peaks were observed for conventional titanium; F1s, Ti2s, O1s, Ti2p3/2, C1s, Ti3s, Ti3p, and O2s peaks were observed for 20 nm diameter anodized nanotubular titanium; and F1s, Ti2s, O1s, Ti2p3/2, C1s, Ti3s, Ti3p peaks were observed for 80 nm diameter anodized nanotubular titanium (Figure 4). The carbon in the outermost layer resulted from the hydrocarbons on the titanium substrates, which was not eliminated even after a vigorous cleaning process (Table 2). Moreover, the presence of fluorine in the top layer of the anodized nanotubular surfaces was attributed to using HF as an electrolyte during the anodization process.

Of course, it has been well established that altering surface chemistry alters cell responses. The influence of fluorine on the surface of the anodized nanotubular titanium clearly may change cell responses compared to unanodized titanium which did not have fluorine on its surface.<sup>15–17</sup> Jin et al<sup>17</sup> claimed that there might be a threshold value for the concentration of fluorine where lower concentrations stimulate the proliferation of certain cells (such as osteoblasts or bone-forming cells) and higher concentrations are toxic for cells. Future studies should create anodized nanotubular titanium without the presence of fluorine (such as by applying heat treatments after the anodization process) to delineate the effect of fluorine on urothelial cells. In addition, different titanium to oxygen ratios between anodized nanotubular and conventional titanium created altered surface chemistry which might also have an impact on the adhesion and proliferation of urothelial cells.

Results of the present study demonstrated that human urothelial cells attached and grew on both conventional and anodized nanotubular titanium plates with culture time (from 4 hours to 1 day to 3 days) (Figure 5). More importantly, compared to conventional titanium, both nanotubular



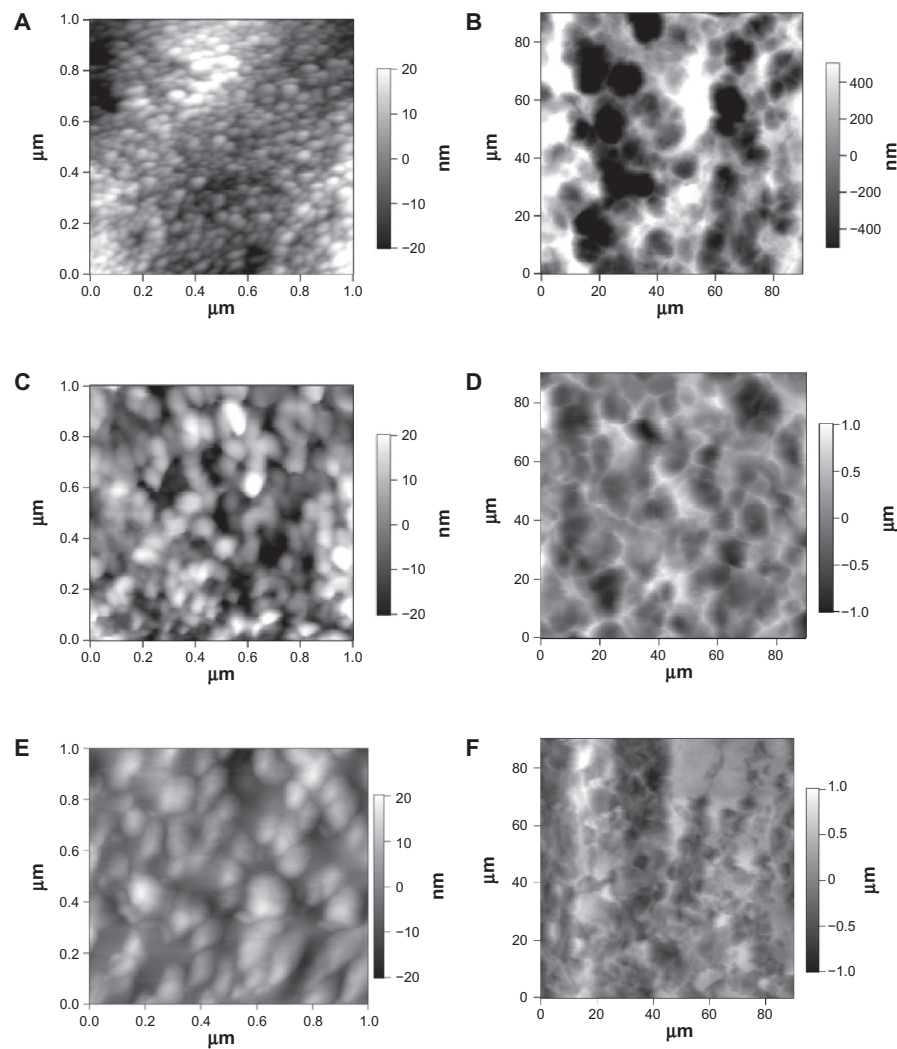


**Figure 3** Atomic force microscopy micrographs showing the topography of **A**) and **B**) 20 nm, **C**) and **D**) 80 nm, and **E**) and **F**) conventional titanium. The images in **A**, **C**), and **E**) show higher magnification scans, highlighting the nanotopography of the samples, and the images in **B**, **D**), and **F**) show lower magnification scans, highlighting the micron-topography of the samples.

titanium samples (20 nm and 80 nm diameter nanotubes) stimulated the attachment of the human urothelial cells after 4 hours. Moreover, urothelial cells proliferated the most on the 20 nm sized nanotubes compared to any other titanium substrate in the present study for up to 3 days.

**Table I** Qualitative data obtained from AFM analysis indicating that substrates created by anodization contained more nanostructured surface features than conventional titanium

| Sample                | rms_nano (nm) | rms_micro (nm) |
|-----------------------|---------------|----------------|
| Anod_20 nm            | 9.97 ± 0.83   | 316.38 ± 18.16 |
| Anod_80 nm            | 9.01 ± 0.40   | 309.53 ± 9.76  |
| Conventional titanium | 6.54 ± 0.37*  | 276.86 ± 9.36  |

**Notes:** Values are mean ± standard error of mean, n = 3; \* $P < 0.01$  compared to all other samples (student t-tests).

**Abbreviation:** AFM, atomic force microscopy.

It is intriguing to wonder why nanotubular titanium improved urothelial cell density in the present study. Along these lines, previous studies have demonstrated increased adsorption of select proteins (specifically, vitronectin, and fibronectin) known to enhance the adhesion of numerous cells (from osteoblasts to endothelial cells).<sup>18</sup> While future studies will need to be conducted to determine if the same events are happening here for urothelial cells, it is highly likely that the increased wettability obtained from anodizing titanium<sup>18</sup> manipulated initial protein adsorption. Future studies will also have to investigate additional functions of urothelial cells (such as select protein synthesis) on the anodized 20 nm diameter nanotubular titanium substrates and why urothelial cell density was improved on the 20 nm compared to 80 nm diameter nanotubular titanium.

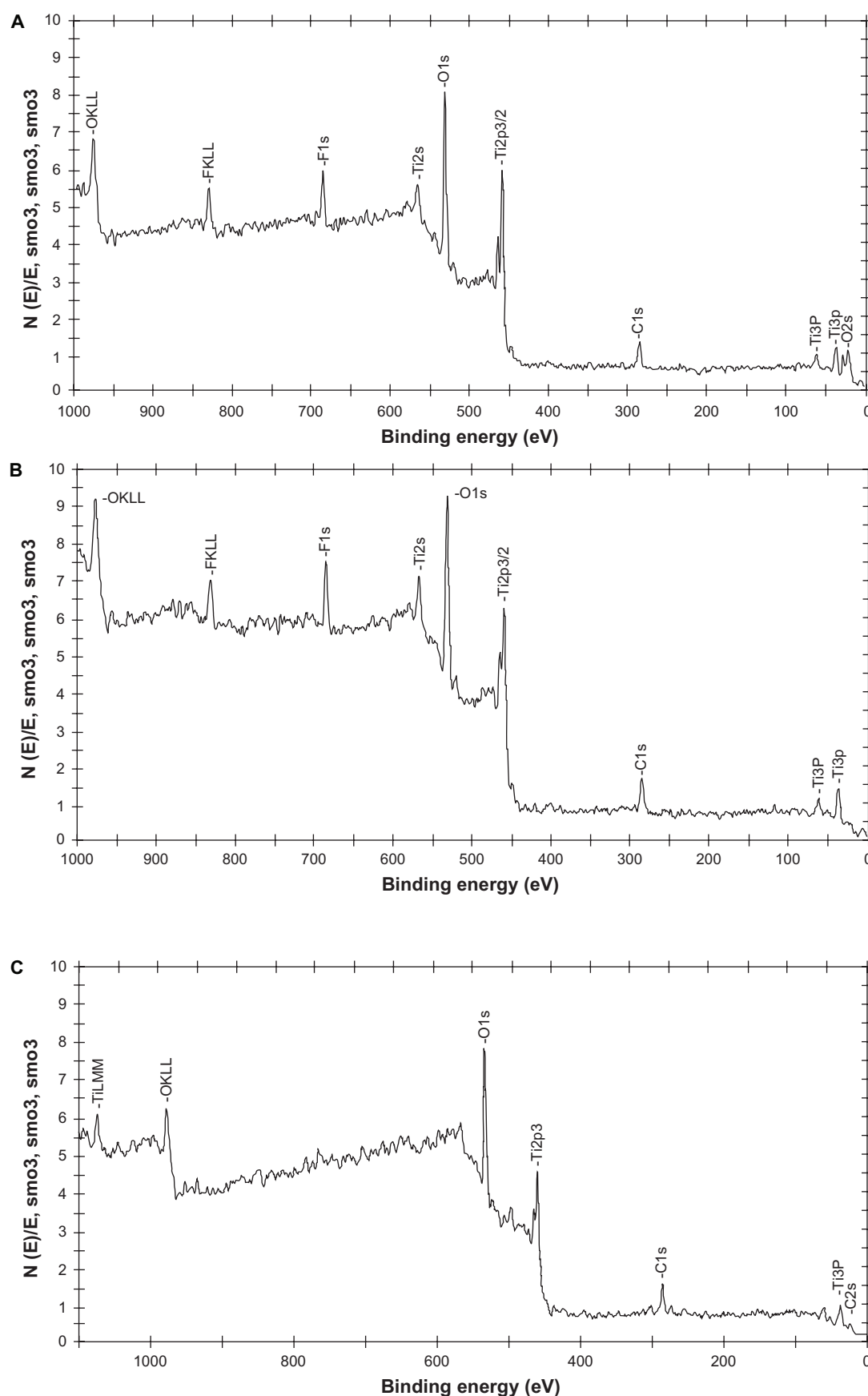


**Figure 4** Electron spectroscopy for chemical analysis for **A)** 20 nm, **B)** 80 nm anodized nanotubular titanium, and **C)** conventional titanium.

**Table 2** Atomic percentages of elements in the outermost layers, as determined by ESCA

| Material (titanium) | Elemental concentration (%) |       |       |       |      |
|---------------------|-----------------------------|-------|-------|-------|------|
|                     | Ti2p                        | O1s   | C1s   | F1s   | Ti/O |
| Conventional        | 19.93                       | 51.29 | 28.79 | 0     | 0.39 |
| Anod_80 nm          | 26.69                       | 40.35 | 21.35 | 11.61 | 0.66 |
| Anod_20 nm          | 22.70                       | 40.21 | 23.50 | 13.59 | 0.56 |

**Notes:** The analysis indicated the presence of fluorine in the outermost layer of anodized samples

**Abbreviations:** ESCA, electron spectroscopy for chemical analysis.

## Conclusions

In summary, results from the present study provided the first evidence that titanium can be modified to possess nanoscale surface features to enhance urothelial cell density, events critical to increase the efficacy of ureter stents. The 20 nm sized nanotubular titanium surfaces provided the best urothelial cell adhesion and proliferation for up to 3 days of any of the titanium samples tested here. In this manner, nanotubular titanium with 20 nm diameters should be further studied for a wide range of bladder applications where urothelialization is desired.

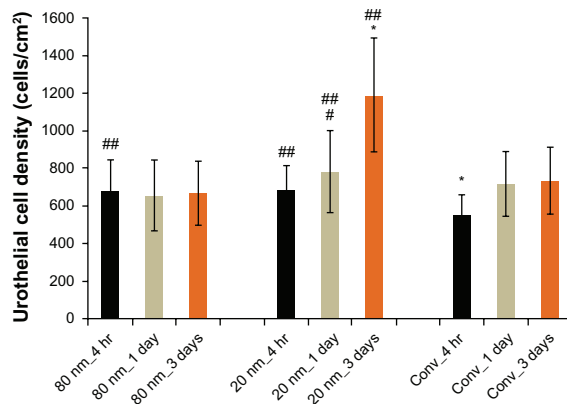


**Figure 5** Urothelial cell densities from 4 hours to 3 days on 20 nm and 80 nm diameter anodized nanotubular titanium, as well as conventional titanium.

**Notes:** Data are mean  $\pm$  SEM  $n = 3$ ; \* $P < 0.01$  compared to respective counterparts at the same time period; # $P < 0.05$  compared to respective sample 4-hour time point; ## $P < 0.05$  compared to conventional titanium at the respective time point. Conv. = conventional titanium. Statistics evaluated using Student  $t$ -tests.

## Acknowledgments

The authors would like to thank the Hermann Foundation for financial support.

## Disclosure

No conflicts of interest were declared in relation to this paper.

## References

- Mardis HK, Kroeger RM. Ureteral stents – materials: endourology update. *Urol Clin North Am*. 1988;15(3):471–479.
- Saltzman B. Ureteral stents – indications, variations and complications: endourology update. *Urol Clin North Am*. 1988;15(3):481–491.
- Chun YW, Khang D, Haberstroh KM, Webster TJ. The role of polymer nanosurface roughness and submicron pores in improving bladder urothelial cell density and inhibiting calcium oxalate stone formation. *Nanotechnology*. 2009;20:1–8.
- Ercan B, Webster TJ. Better tissue engineering materials through the use of nanotechnology. *Adv Sci Technol*. 2006;53:58–66.
- Nel AE, Madler L, Velegol D, et al. Understanding biophysochemical interactions at the nano–bio interface. *Nat Mater*. 2009;8:543–557.
- Champion JA, Mitragotri S. Role of target geometry in phagocytosis. *Proc Natl Acad Sci U S A*. 2006;103:4930–4934.
- Gratton SEA, Ropp PA, Pohlhaus PD, et al. The effect of particle design on cellular internalization pathways. *Proc Natl Acad Sci U S A*. 2008;105:11613–11618.
- Choi HS, Liu W, Liu F, et al. Design considerations for tumour-targeted nanoparticles. *Nat Nanotechnol*. 2009;5:42–47.
- Delehanty JB, Mattoussi H, Medintz IL. Delivering quantum dots into cells: strategies, progress and remaining issues. *Anal Bioanal Chem*. 2009;393:1091–1105.
- Huff TB, Hansen MN, Zhao Y, Cheng J-X, Wei A. Controlling the cellular uptake of gold nanorods. *Langmuir*. 2007;23:1596–1599.
- Park S, Hamad-Schifferli K. Nanoscale interfaces to biology. *Curr Opin Chem Biol*. 2010;14:1–7.
- Lee WJ, Alhoshan M, Smyrl WH. Titanium dioxide nanotube arrays fabricated by anodizing processes. *J Electrochem Soc*. 2006;153(11):B499–B505.
- Kim HS, Yang Y, Koh JT, et al. Fabrication and characterization of functionally graded nano-micro porous titanium surface by anodizing. *J Biomed Mater Res B*. 2009;88(2):427–435.
- Park J, Bauer S, Schlegel KA, Neukam FW, Mark KVD, Schmuki P. TiO<sub>2</sub> nanotube surfaces: 15 nm – an optimal length scale of surface topography for cell adhesion and differentiation. *Small*. 2009;5(6):666–671.
- Yan X, Feng C, Chen Q, et al. Effect of sodium fluoride treatment in vitro on cell proliferation, apoptosis and caspase-3 and caspase-9 mRNA expression by neonatal rat osteoblasts. *Arch Toxicol*. 2009;83:451–458.
- Wang Y, Zhang S, Zeng X, et al. Osteoblastic cell response on fluoride-treated hydroxyapatite coatings. *Acta Biomater*. 2007;3:191–197.
- Jin XQ, Xu H, Shi HY, Zhang JM, Zhang HQ. Fluoride-induced oxidative stress of osteoblasts and protective effects of baicalin against fluoride toxicity. *Biol Trace Elem Res*. 2007;116:81–89.
- Yao C, Slamovich EB, Webster TJ. Enhanced osteoblast functions on anodized titanium with nano-tube like structures. *J Biomed Mater Res B*. 2007;85A(1):157–166.